Disordered Protein Stabilization by Co-Assembly of Short Peptides Enables Formation of Robust Membranes

Journal:	*ACS Applied Materials & Interfaces*
Manuscript ID	Draft
Manuscript Type:	Article
Date Submitted by the Author:	n/a
Complete List of Authors:	Ghosh, Moumita; Tel Aviv University, Sackler Faculty of medicine, The Goldschleger School of Dental Medicine, Department of Oral Biology Majkowska, Anna; Queen Mary University of London misra, rajkumar; Tel Aviv University, Bera, Santu; Tel Aviv University Faculty of Social Sciences, Molecular Microbiology and Biotechnology Department Rodriguez-Cabello, Jose Carlos; University of Valladolid Mata, Alvaro; University of Nottingham, Adler-Abramovich, Lihi; Tel Aviv University, Department of Oral Biology, The Goldschleger School of Dental Medicine Sackler Faculty of Medicine

SCHOLARONE™
Manuscripts

Disordered Protein Stabilization by Co-Assembly of Short Peptides Enables Formation of Robust Membranes

Moumita Ghosh[1,2,3], Anna Majkowska[4,5], Rajkumar Mirsa[1,2], Santu Bera[1,2], José Carlos Rodriguez-Cabello[6], Alvaro Mata[7,8,9], and Lihi Adler-Abramovich[1,2]*

[1]Department of Oral Biology, The Goldschleger School of Dental Medicine, Sackler Faculty of Medicine, Tel-Aviv University 69978, Israel.

[2]The Centre for Nanoscience and Nanotechnology, Tel Aviv University, Tel Aviv, 6997801 Israel

[3]Department of Chemistry, Techno India University, EM-4, EM Block, Sector V, Bidhannagar, Kolkata, West Bengal 700091, India.

[4]School of Engineering & Materials Science, Queen Mary University of London, London E1 4NS, U.K.

[5]William Harvey Research Institute, Queen Mary University of London, London, EC1M 6BQ, UK

[6]BIOFORGE Group, University of Valladolid, CIBER-BBN, Valladolid 47011, Spain.

[7]School of Pharmacy, University of Nottingham, Nottingham NG7 2RD, UK.

[8]Department of Chemical and Environmental Engineering, University of Nottingham, Nottingham NG7 2RD, UK.

[9]Biodiscovery Institute, University of Nottingham, Nottingham NG7 2RD, UK.

*Correspondence to: LihiA@tauex.tau.ac.il

1

ABSTRACT

Molecular self-assembly is a spontaneous natural process resulting in highly ordered nano- to micro-architectures. We report temperature-independent formation of robust stable membranes obtained by spontaneous interaction of intrinsically disordered elastin-like polypeptides (ELPs) with short aromatic peptides at temperatures both below and above the conformational transition temperature of the ELPs. The membranes are stable over time and display durability over a wide range of parameters including temperature, pH, and ultrasound energy. The morphology and composition of the membranes was analysed using microscopy. These robust structures support preosteoblast cell adhesion and proliferation as well as pH-dependent cargo release. Simple non-covalent interactions with short aromatic peptides can overcome conformational restrictions due to phase transition, to facilitate formation of complex bioactive scaffolds that are stable over a wide range of environmental parameters. This approach offers novel possibilities for controlling conformational restriction of intrinsically disordered proteins and using them in the design of new materials.

Keywords: Intrinsically disordered proteins, Co-assembly, Short peptides, Membranes, Biocompatible.

61 **INTRODUCTION**

62 Studies in the field of molecular self-assembly have led to the development of a variety of new

63 bioinspired three-dimensional (3D) materials with enhanced complexity and dynamic

64 properties. Proteins represent a rich source of building blocks for molecular self-assembly, due

65 to their versatility and bio-functionality, and their use has enabled the formation of highly

66 ordered architectures, which can be utilized as cellular structures, support elements, or

67 connective tissues.[1-2] These naturally occurring complex architectures possess excellent

68 capabilities for self-healing, hierarchical order, adaptability, and bioactivity. In the last two

69 decades, much attention has been devoted to the design of a wide variety of self-assembling

70 supramolecular functional structures based on naturally occurring proteins, including

71 collagens, elastin, silk, and keratin. These structures play a central role in bottom-up

72 nanotechnology and have the potential to be used as hydrogel scaffolds, biomimetic cellular

73 support structures, membranes, and drug delivery vehicles. [3-7]

74 In nature, proteins undergo conformational transitions from disordered-to-ordered states which

75 are fundamental to all biological functions.[8,9] The 3D structures of proteins are often partially

76 or completely disordered in their natural environment and may undergo significant

77 transformations. This phenomenon recently attracted much attention, when a notable number

78 of proteins were shown to contain large intrinsically disordered regions, which are devoid of a

79 well-defined structure in solution. These areas assume an organized conformation only when a

80 specific function is required. For example, when binding to other proteins in order to fulfil key

81 regulatory functions, in transcription and translation, protein phosphorylation, or cellular signal

82 transduction, as well as mechanical roles. This natural phenomenon has inspired the design of

83 new materials with unique and promising properties due to their ability to undergo dynamic

84 phase transitions in response to environmental triggers.[10,11] Unfortunately, the flexibility of the

85 structures tends to limit their stability and complicates their use for engineering applications

86   that require reproducibility. Any thermally triggered changes in the environment may cause the

87   segments of the intrinsically disordered proteins (IDPs) to stick together or break apart,

88   resulting in a phase transition from a stable to an unstable state.[11-13] One approach to overcome

89   this limitation, would be to design molecules with a favourable equilibrium between

90   association and dissociation. For example, elastin-like polypeptides (ELPs), a class of stimuli-

91   responsive biopolymers inspired by the intrinsically disordered domains of tropoelastin, are

92   composed of repeats of the VPGXG pentapeptide motif, in which X is any amino acid except

93   proline.[14,15] Proteins of this type possess a modular structure, bioactivity, and an ease of design

94   and production that offer possibilities of producing materials applicable for protein

95   purification, affinity capture, immunoassays, and drug delivery.[16,17] ELPs can also serve as a

96   model of IDPs and hence can provide insights into the behaviour of other more complex

97   molecules.

98

99   The capacity to fabricate robust functional materials with ELPs, and more broadly, with other

100   IDPs, is often limited by the difficulty of controlling the intermolecular non-covalent

101   interactions and structural complexity. Supramolecular chemistry offers a tool to control

102   protein function and to develop materials with new synergistic properties. Peptide

103   supramolecular assembly has been effectively utilized to produce materials with functional

104   properties for various applications, including tissue engineering scaffolds, encapsulation and

105   slow release of drugs and biomolecules, templates for nanofabrication, and catalysts for organic

106   reactions.[18-24] Even molecules as small as dipeptides, can be designed with all the molecular

107   information needed for spontaneous formation of well-ordered structures at both the nano and

108   the micro-scale.[18-20,25,26]

109   The prospect of being able to expand the range of applications has aroused much recent interest

110   in multicomponent peptide supramolecular systems.[27] This is particularly interestingly since,

111 in most cases, co-assembled systems exhibit properties that are superior to those of the

112 individual building blocks.[27-34] Examples include materials where the nanostructure can be

113 modified to form non-canonical complex topologies[27,28,33], modulate mechanical

114 properties[29,30,34], and even access out-of-equilibrium processes to enable the capacity to grow

115 or self-heal.[17,35] Such materials have been used in the design of light harvesting soft materials[36],

116 fabrication of electrically conducting devices[37,38], induced fluorescence[39], enzymatic

117 catalysis[40], fabrication of *in vitro* models[41], and tissue engineering.[34,42] One interesting class of

118 co-assembled peptide system, enables the formation of macroscopic sacs, membranes, and

119 nanofibers at the interface between two aqueous solutions, where one solution contains a

120 peptide amphiphile (PA), and the other contains a high molecular weight polymer with the

121 opposite charge.[43-45] However, more complex protein structures that include both ordered and

122 disordered regions being more functional, can provide more flexibility to the overall

123 supramolecular arrangement. The mechanical and chemical properties of such protein-based

124 materials can be manipulated by the selection of constituent amino acids that are capable of

125 responding to temperature, electrical, magnetic, or enzymatic stimuli, which gives them an

126 advantage over polysaccharides. The introduction of PAs into an aqueous solution of ELPs and

127 resilin has been shown to trigger a diffusion reaction mechanism resulting in a multi-layered

128 membrane with the capacity to dis-assemble controllably, seal to interfaces, self-heal, and

129 undergo controlled morphogenesis into complex tubular networks.[17,46,47] In another study,

130 model IDPs, have shown its capacity to hierarchically self-organise into micrometer-size

131 biomorphs with complex shapes.[48] Notably however, these systems remain dependent on the

132 presence of inherent disordered structures, which tends to limited functionality. There is

133 therefore still an unmet need to identify an optimum system in which the disorder can be

134 controlled and stabilized, in order to obtain more practical and predictable materials.

135 Here, we describe the synthesis of novel membranes with an extended shelf life that are co-

136 assembled from an ELP and a short aromatic peptide. As a modification of the system, cell

137 adhesive RGDS motifs were included in the negatively charged ELPs, and the short tri-peptide,

138 Fmoc-Phe-Phe-Lys, was designed with an overall positive charge. Interestingly, interfacial

139 self-assembled macroscopic systems develop spontaneously above and, more surprisingly, also

140 below the transition temperature (T_t) of the ELP. These systems are stable over a wide range

141 of pH, and temperatures, are resistant to sonication, and remain durable over time. The

142 morphology of the membranes formed in the self-assembled stable systems was characterized

143 using optical, scanning electron, and fluorescent confocal microscopy, and was found to

144 contain nanofibrous assemblies. The self-assembled systems formed are biocompatible with

145 MC3T3-E1 preosteoblast cells, which adhere well to the membranes. The membranes can also

146 encapsulate and release dye in a pH-dependent fashion. Short aromatic peptides with their

147 intrinsic optimum hydrophilic and lipophilic balance can interact with both ordered and

148 disordered forms of the protein, thus overcoming the problems of phase transition and

149 producing robust macroscale hybrids. This simple system represents a new approach for

150 controlling disordered proteins, with new possibilities for utilization in material design.

151

RESULT AND DISCUSSIONS

153 **Protein-peptide membrane formation.** We studied the ELP5 co-assembly with Fmoc-

154 protected peptide. The ELP5 is a long pentablock molecule with distinct hydrophobic domains,

155 which undergoes a phase transition and evolves into a collapsed conformation in an aqueous

156 environment above the T_t of 19 °C.[17] It is negatively charged above the isoelectric point of 3.4.

157 Four of the five blocks are based on the elastin sequence VPGXG, with X being isoleucine (I),

158 valine (V), or glutamic acid (E), while the fifth block contains an Arg-Gly-Asp-Ser (RGDS)

159 motif to promote cell adhesion (Figure 1A). The Fmoc-protected peptide contains two

160 phenylalanine residues attached to hydrophilic lysine residue that imparts an overall positive

161 charge to the peptide segment (Figure 1B).
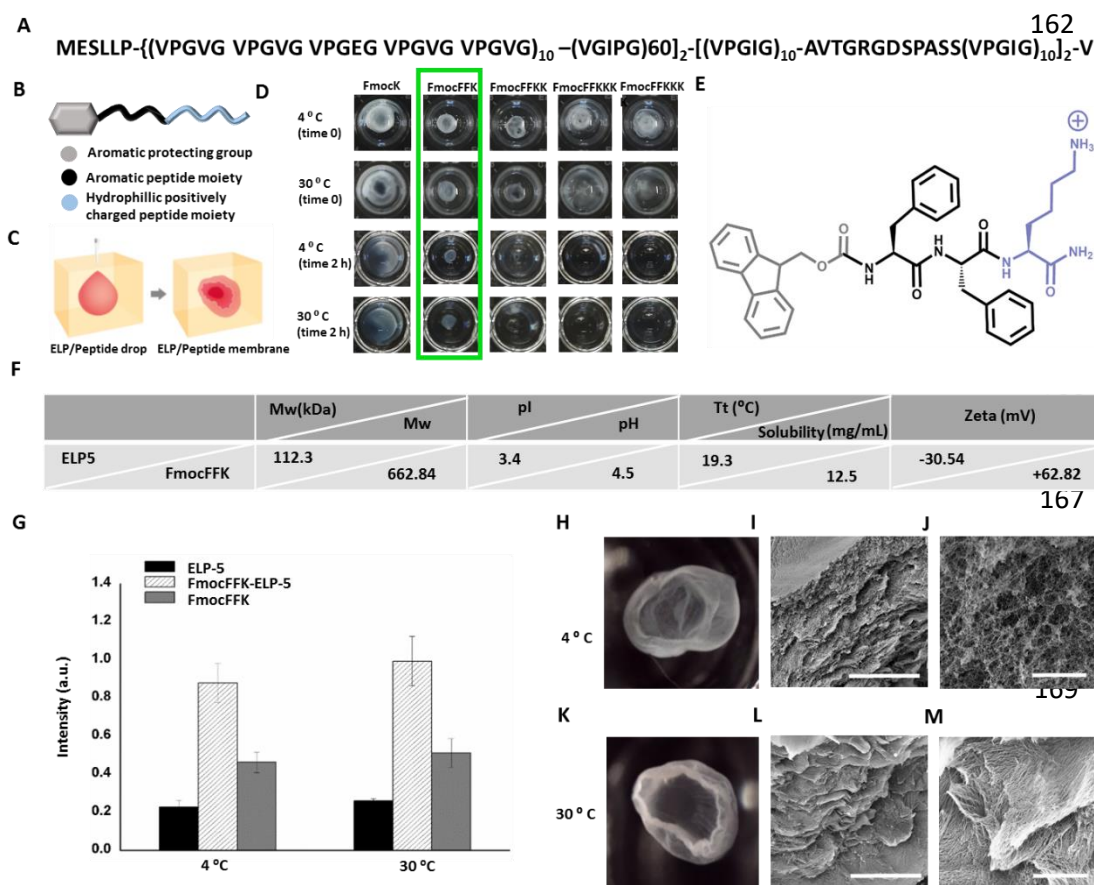
Figure 1. Peptide-polymer membranes. (A) Structure of ELP, (B) Representation of the short aromatic peptides used, (C) Time-lapse schematic representation of the self-assembly of a ELP5-peptide membrane where the peptide solution was immersed in a larger volume of ELP5 solution (D) Formation of self-assembled structures on immersion of different peptide solutions in ELP5 solution at 4^{0}C or 30^{0}C; immediately after exposure and after two hours, (E) Structure of Fmoc-Phe-Phe-lysine, which forms a membrane on immersion in ELP solution, (F) A table showing the physical properties of ELP5 and FmocFFK, (G) Turbidity profile of solutions of peptide and ELP5 at 300 nm demonstrate the requirement for the self-assembly process to take place either above or below the ELP5 transition temperature because of hydrophobic interactions between the two molecules, (H) Optical microscopy image of the ELP5- FmocFFK membrane formed at 4^{0}C. Scale bar represents 500 μm, (I, J) Scanning electron microscopy image showing the multilayer and fibrillar morphology of the membrane formed at 4^{0}C. Scale bars represents 50 μm and 10 μm respectively (K) Optical microscopy image of the ELP5-FmocFFK membrane formed at 30^{0}C. Scale bar represents 500 μm (L, M) Scanning electron microscopy image showing the multilayer and fibrillary morphology of the membrane formed at 30^{0}C, scale bars represents 50 μm and 10 μm respectively.

7

172   For this study, five peptide sequences with a gradual increase in the hydrophilicity and positive

173   charge were designed: namely Fmoc-Lys (FmocK), Fmoc-Phe-Phe-Lys (FmocFFK), Fmoc-

174   Phe-Phe-Lys-Lys (FmocFFKK), Fmoc-Phe-Phe-Lys-Lys-Lys (FmocFFKKK), and Fmoc-Phe-

175   Phe-Lys-Lys-Lys-Lys (FmocFFKKKK) (Figure S1). A small amount of peptide aqueous

176   solution (10 μL) was immersed in a large bulk volume (100 μL) of 1% (wt) ELP5 at 4^0C and

177   30^0C (below and above the T_t (19°C)), respectively, (Figure 1C). Following the addition of

178   ELP5, all the peptides exhibited a spontaneous interfacial self-assembly (Figure 1D). While

179   the systems composed of FmocK, FmocFFKK, FmocFFKKK and FmocFFKKKK

180   disintegrated after 2 h at both temperatures, FmocFFK in ELP5 produced a well-defined

181   durable membrane (Figure 1D). The durable membrane is the result of FmocFFK optimum

182   hydrophilic-lipophilic balance, with a positive zeta potential of +62.82 mV, that can form an

183   interfacial surface with the negatively charged ELP5 (Figure 1E, F). The absence of a

184   hydrophobic FF moiety in FmocK, resulted in a lack of hydrophilic-lipophilic balance in the

185   interaction between ELP5 and FmocK, thus no well-defined structures were formed. On the

186   other hand, the large charge density of FmocFFKK, FmocFFKKK and FmocFFKKKK also

187   failed to meet the optimum hydrophilic-lipophilic balance required for membrane formation.

188   Hence, the optimum hydrophilic-lipophilic balance of FmocFFK made it the most suitable

189   candidate in the peptide library to interact with ELP5 and form a stable membrane. Increasing

190   the concentration of the peptide from 2.26 mM to 18.85 mM (the maximum water solubility),

191   while maintaining a fixed concentration of ELP5, produced a robust membrane, which

192   ultimately formed an open sac-like structure at 18.85 mM peptide (Figure S2). The sacs became

193   more robust after 24 hours and could be handled with tweezers both in water and air (Figure

194   S3). We assume that the conformational modification that exposes the hydrophobic domain of

195   ELP5, together with electrostatic interactions between the oppositely charged ELP5 and the

196   peptide molecules, resulted in a dynamic self-assembling process[16,17]. Interestingly, while

197 interactions that results in the formation of PA-ELP sacs were previously observed only above

198 the T_t[17], here we observed a dynamic self-assembled phenomenon from membrane to sac

199 formation also at 4^0C, which is below the 19° C T_t of ELP5 (Figure 1D). To verify this

200 temperature independence and investigate the interactions present in the ELP5-FmocFFK

201 system, turbidity analysis was conducted both above and below the T_t (Figure 1G). The

202 turbidity profile of 0.01 mM ELP5 and 0.18 mM peptide solutions measured at 300 nm,

203 exhibited significant aggregation at temperatures both below and above the T_t. Interestingly,

204 the optical density of the combined system was much higher than that of the individual

205 components (Figure 1G).

206 The macroscopic structures formed both above and below the T_t appeared very similar (Figure

207 1 H,K). This is in contrast to the results of previous studies with peptide amphiphiles, where

208 the PAs conformation of the ELP5 molecules played a critical role in the co-assembling process

209 and resulting material properties[17]. We assume that the small dimensions of the short FmocFFK

210 tripeptides can improve its flexibility and penetration of the peptide into the protein domain,

211 therefore affecting the equilibrium between order and disorder at T_t and leading to the

212 formation of macroscopic ordered structures even at lower temperatures (Figure 1H, K).

213 Scanning electron microscopy (SEM) analysis of the protein/peptide sac membranes formed

214 overnight both below and above the T_t (Figure 1 I, J, L, M) revealed a nanofibrous multi-

215 layered membrane structure. The fibrils were several micrometers long and ~100 nm in

216 diameter. Interestingly, the fibrils appeared more aligned in the structure formed above the T_t

217 than in material formed below the T_t (Figure 1 I, J, L, and M). This morphological difference

218 between the two systems might be the result of a different conformational orientation of the

219 ELP5 molecule at the different temperatures. Transmission electron microscopy images of the

220 peptide aqueous solution at both 4 °C and 30 °C showed that the peptide itself can self-assemble

221 into several micrometers long fibrils (Figure S4). Furthermore, the secondary structure of the

222   pristine peptide was observed to be β-sheet at both circular dichroism with characteristic peak

223   at 218-224 nm, and Fourier-transform infrared spectroscopy analysis with characteristic peak

224   at 1682 cm^{-1} and 1637 cm^{-1}. Similar secondary structure was observed in pH 2, 7 and 14.

225   (Figure S5). This peptide orientation as well as its self-assembling fibrils property might have

226   contributed to the multi-layered fibrillary features of the membranes.

227

228   **Microscopic characterization of the ELP5-FmocFFK membranes.** The localization of the

229   individual components in the macrostructure was investigated by confocal microscopy (Figure

230   2). ELP5 in aqueous solution was labeled with Alexa Fluor green and the peptide solution was

231   labeled with the red dye rhodamine. Membranes were prepared from 1% wt ELP5 and 18.85

232   mM peptide. Interestingly, the merged images revealed that membranes formed below the T_t,

233   ELP5 (green) is present both at the boundary and inside the membrane (Figure 2A-D), but at

234   membranes formed above the T_t, the ELP is seen only at the boundary of the membranes (Figure

235   2E-H). Time of flight-secondary-ion mass spectrometry (TOF-SIMS) analysis used the

236 positive secondary ion C4H8N+ 70 m/z to identify ELP5 and the positive ion C14H11+ 179

237 m/z to identify FmocFFK (Figure S6). The results of the ToF-SIMS revealed an abundance of

238 ELP5 in the boundary of the membranes formed at 30 ^{0}C, while at 4 ^{0}C both ELP5 and

239 FmocFFK were localized at the boundary of membranes formed (Figure 2I, K). These results

240 were
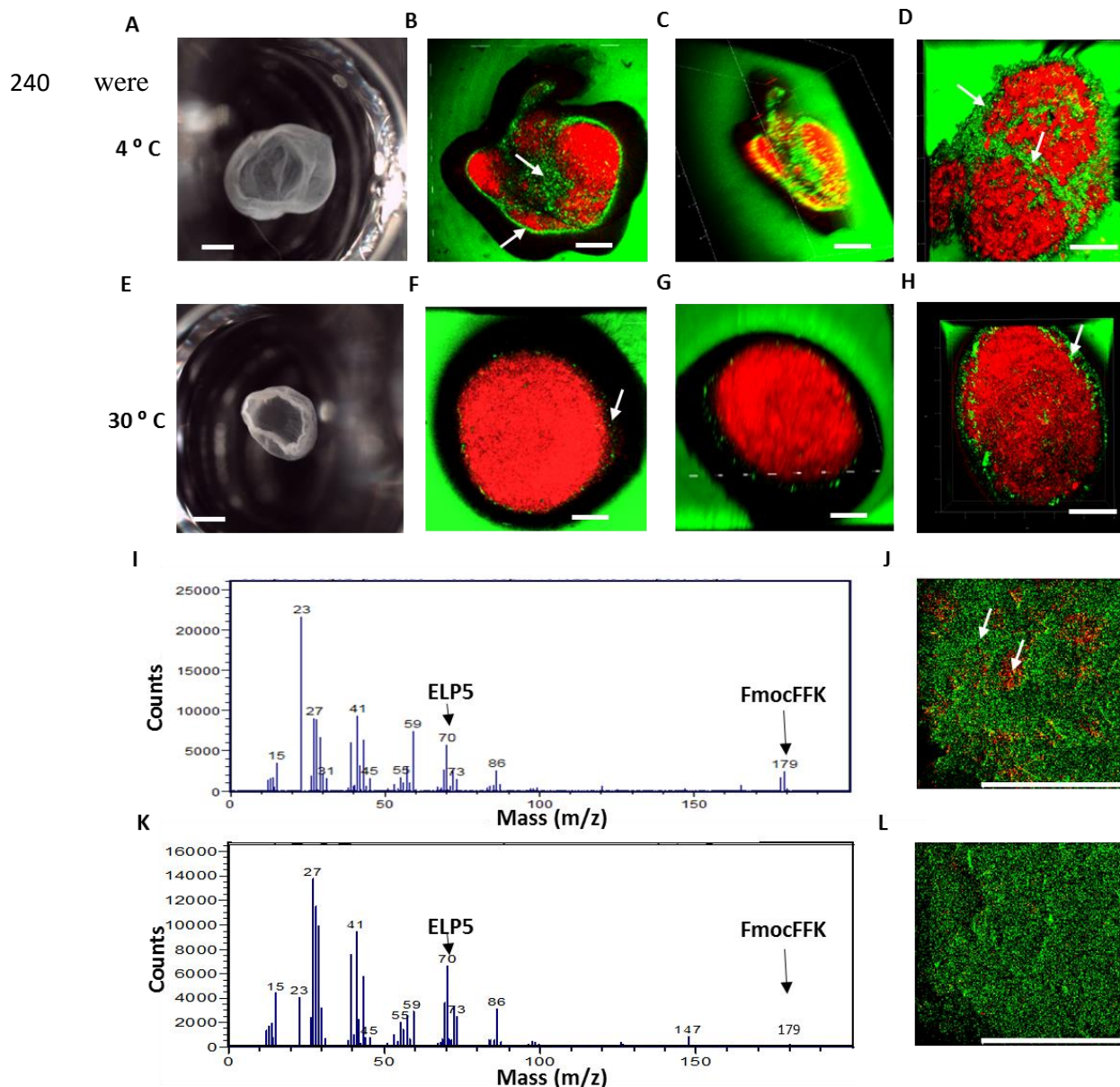
Figure 2. Microscopic and ToF-SIMS characterization of peptide-polymer membranes. (A) Optical images of ELP5-FmocFFK membranes formed at 4^{0}C, scale bar represents 500 μm, (B, C, D) Confocal microscopy image of membranes formed at 4^{0}C showing the localization of ELP5 (stained with green dye) and peptide (stained with red dye), scale bar represents 500 μm, (E) Optical images of ELP5-FmocFFK membranes formed at 30^{0}C, scale bar represents 500 μm, (F, G, H) Confocal microscopy image of membranes formed at 30^{0}C showing the localization of ELP5 (stained with green dye) and peptide (stained with red dye), scale bar represents 500 μm, ToF-SIMS Mass spectrometry analysis of ELP5-FmocFFK membranes formed at (I) 4^{0}C and (K) 30^{0}C. Chemical ion maps of ELP5-FmocFFK membranes formed at (J) 4^{0}C and (L) 30^{0}C. Scale bar represents 100 μm.

241 validated by chemical ion mapping in which different colors were assigned to specific ions

242 from the mass spectra and their location in a precise area of the boundary of each membrane

243 was observed. The FmocFFK- C14H11+ 179 m/z were marked in red and ELP5-C4H8N+ 70

244 m/z were marked in green. The pattern of green and red dots over the mapped area confirms

245 the presence of both C14H11+ 179 m/z (red) and C4H8N+ 70 m/z (green) at the boundary of

246 membranes formed at 4^0C, while the boundary of membranes formed at 30^0C contains an

247 abundance of C4H8N+ 70 m/z (green) (Figure 2J, L). The differences in the localization of the

248 two components in membranes formed at the two different temperatures can be attributed to

249 the different conformations adopted by ELP5 under these conditions.

250

251 **Stability analysis of the ELP5-FmocFFK membranes.** In order to examine the stability of

252 the ELP5-FmocFFK membranes formed at the two temperatures, the membranes were exposed

Table 1. Stability of the peptide-polymer membranes. (A) Stability of the membranes prepared at 4^0C and 30^0C, over a temperature range of 2^0C to 100^0C, (B) Stability of the membranes prepared at 4^0C and 30^0C to sonication for between 5 to 30 mins.

A

Temperature	0°C	20°C	40°C	60°C	80°C	100°C
Membrane Formed at 30°C	Stable	Stable	Stable	Stable	Stable	Stable
Membrane Formed at 4°C	Stable	Stable	Stable	Stable	Disintegrated	Disintegrated

B

Sonication time	0 min	5 min	10 min	20 min	30 min
Membrane Formed at 30°C	Stable	Stable	Stable	Stable	Disintegrated
Membrane Formed at 4°C	Stable	Stable	Stable	Disintegrated	Disintegrated

253   to a various environmental conditions, such as different temperatures, pH, and sonication.

254   Membranes formed above or below the T_t appeared quite stable after a 48 h incubation in buffer

255   solutions with a pH ranging from pH 2-14 (Figure S7), although at acid pH they membranes

256   were observed to be more opaque and at basic pH more transparent. Rheological measurements

257   to characterize the effect of pH on the mechanical properties of the membranes revealed a

258   change in the storage modulus of the membranes exposed to 0.01-100% strain at a constant

259   frequency of 1 Hz. Interestingly, membranes formed at 30^0 C (305 Pa) displayed a slightly

260   higher storage modulus than those formed at 4^0C (104 Pa) (Figure S8A, B). However, in both

261   cases, membranes immersed in acidic pH (pH 2) were more rigid than membranes incubated

262   at neutral (pH 7) (102 Pa for membrane at 30 ^{0}C and 73 Pa for 4 ^{0}C) or basic pH (pH 14) (72

263   Pa for membrane at 30^0 C and 41 Pa for 4^0 C), Figure S8A, B). Considering the charge

264   distribution of ELP and the peptide in acidic pH, it is indeed possible that in addition to the

265   electrostatic forces, other factors such as hydrophobic interactions and π-π stacking between

266   the aromatic moieties, play a significant role in the enhanced rigidity of the membranes at pH

267   2. All the membranes were prepared both at 4 °C and 30 ^{0}C at acidic, neutral and basic pH

268   displayed a gel-like nature, as observed from their strain sweep analysis, showing that the

269   storage modulus (G') was higher than the loss modulus (G'') (Figure S9). SEM analysis

270   demonstrated that the fibrillar morphology of both the membrane prepared at 4 and 30 ^{0}C was

271   found to be intact at all the pH range acidic (pH 2), neutral (pH 7) and basic (pH 14) (Figure

272   S10).

273   Thus, the apparent opacity of the membranes in acidic pH compared to those in neutral (pH 7)

274   or basic pH (pH 14) could be related to the increase in rigidity. All the membranes

275   demonstrated a high storage modulus up to a strain of 5%, but there was subsequently a gradual

276   decline with increased strain (Figure S8A, B). Table 1A, (Figure S11) presents evidence for

277   the stability of the ELP5-FmocFFK membranes over a range of temperatures. Membranes

278   formed at 30^0C were stable from 2 -100^0C, although above 80^0C the solution started to become

279   turbid, probably due to some partial-degeneration of the membrane. In contrast, membranes

280   formed at 4^0C were stable up to 60^0C, but completely disintegrated and dissolved at higher

281   temperatures (Table 1A, Figure S11). The stability of sonicated membranes is presented in

282   Table 1B (Figure S12). Although membranes formed at 4 ^{0}C were stable up to 10 mins of

283   sonication, those formed at 30 ^{0}C could withstand up to 20 mins of sonication before signs of

284   degeneration were observed. In conclusion, our results suggest that the ELP5-FmocFFK

285   membranes formed at 30 ^{0}C are mechanically stronger and more resistant to temperature and

286   sonication than those formed at 4 ^{0}C. The turbidity profile of the aqueous layer above the

287   membrane prepared at 4 and 30 ^{0}C with respect to the temperature also supported the fact that

288   at the high temperature the solution became turbid with an OD value of 0.5 at 305 nm indicating

289   the dissolution of the membranes. Similar observations were noticed for membranes prepared

290   at 4 and 30 ^{0}C, with high sonication time resulting in OD values of 0.5 (Figure S13).

291   **Application of ELP5-FmocFFK membranes in tissue engineering.** Following the

292   microscopic and mechanical characterization of the protein-peptide membrane systems formed

293   at two different temperatures, cytocompatibility and effect on cells was evaluated. MC3T3-E1

294   preosteoblast cells were used as a model. Membranes formed both above and below the T_t were

295   stable in cell culture medium for 7 days without any evidence of deformation (Figure S14).

296   Cells seeded on the top side of pre-washed membranes were stained with fluorescein

297   isothiocyanate (green) to visualize the localization of live cells on the membrane. MC3T3-E1

298   cells could be seen both inside and outside the surface of the membranes prepared at 4 ^{o}C, but

299   appeared exclusively at the outside surface of membranes prepared at 30 ^{0}C (above T_t, Figure

300   3A, B, D, E). To verify these results, the membrane was stained with rhodamine (red) and the

301   cells with DAPI (blue). As expected, cells stained with DAPI were present both inside and at

302   the boundary of the membranes formed at 4 ^{0}C, but only at the boundary of membranes formed

303   at 30 ^{0}C (Figure 3C, F). This pattern of localization of the cells is reminiscent of the observed

304   presence of ELP in the membranes formed above or below the T_t. Since ELP5 contains the

305   RGDS moiety, which is known for its cell binding property it is reasonable to suppose that this

306   could be the reason for the cellular behaviour. Fluorescence microscopy showed that the cells

307   maintain good morphology on the surface of the membranes prepared both above and below

308   T_t, which confirms the ability of the membranes to support cellular growth and proliferation of

309   MC3T3-E1 cells. SEM images obtained 3 days after seeding MC3T3-E1 cells on the surface

310   of the membranes both the above and below T_t prepared membranes show well distributed cell

311   growth (Figure 3G, H, Figure S15). Cells anchored to the membranes could be seen to interact
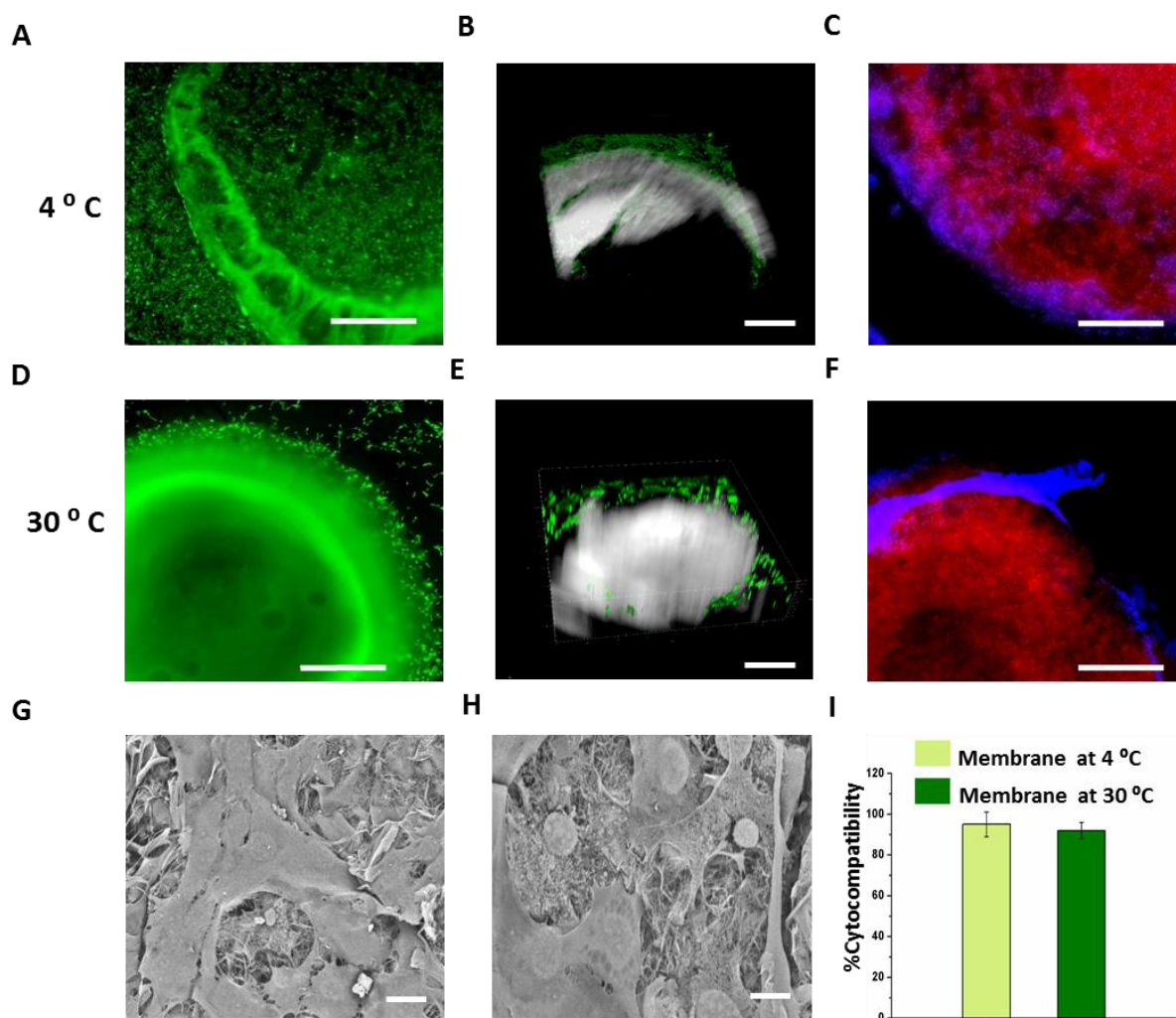
Figure 3. In vitro biocompatibility of peptide-polymer membranes. MC3T3-E1 preosteoblast cell growth and proliferation on the membranes after 3 days (cells stained with fluorescein diacetate dye) (A) Fluorescence optical image of membranes formed at 4^{0}C showing the localization of live cells on the membrane, (B) Confocal microscopic image of membranes formed at 4^{0}C showing the localization of live cells on the membrane (C) MC3T3-E1 preosteoblast cell localization on membranes formed at 4^{0}C after 3 days (cells stained with DAPI, membrane stained with rhodamine dye). MC3T3-E1 preosteoblast cell growth and proliferation on the membranes after 3 days (cells stained with fluorescein diacetate dye) (D) Fluorescence optical image of membranes formed at 30°C showing the localization of live cells on the membrane, (E) Confocal microscopic image of membranes formed at 30^{0}C showing the localization of live cells on the membrane, (F) MC3T3-E1 preosteoblast cell localization on membranes formed at 30^{0}C after 3 days (cells stained with DAPI, membrane stained with rhodamine dye). Scanning electron microscopy image showing cell anchoring in the fibrillar matrix of the membranes prepared at (G) 4 ^{0}C, (H) 30 ^{0}C, (I) MTT assay performed on the membranes prepared at 4 ^{0}C and 30 ^{0}C showing the cytocompatibility of the membranes. Scale bar represents 500 μm.

312   extensively with the fibrillar morphology of the membranes. These results confirm that the

313   ELP/peptide membranes formed above or below the Tt can support cell adherence, growth, and

314   proliferation and thus have potential for use in tissue engineering. We evaluated the
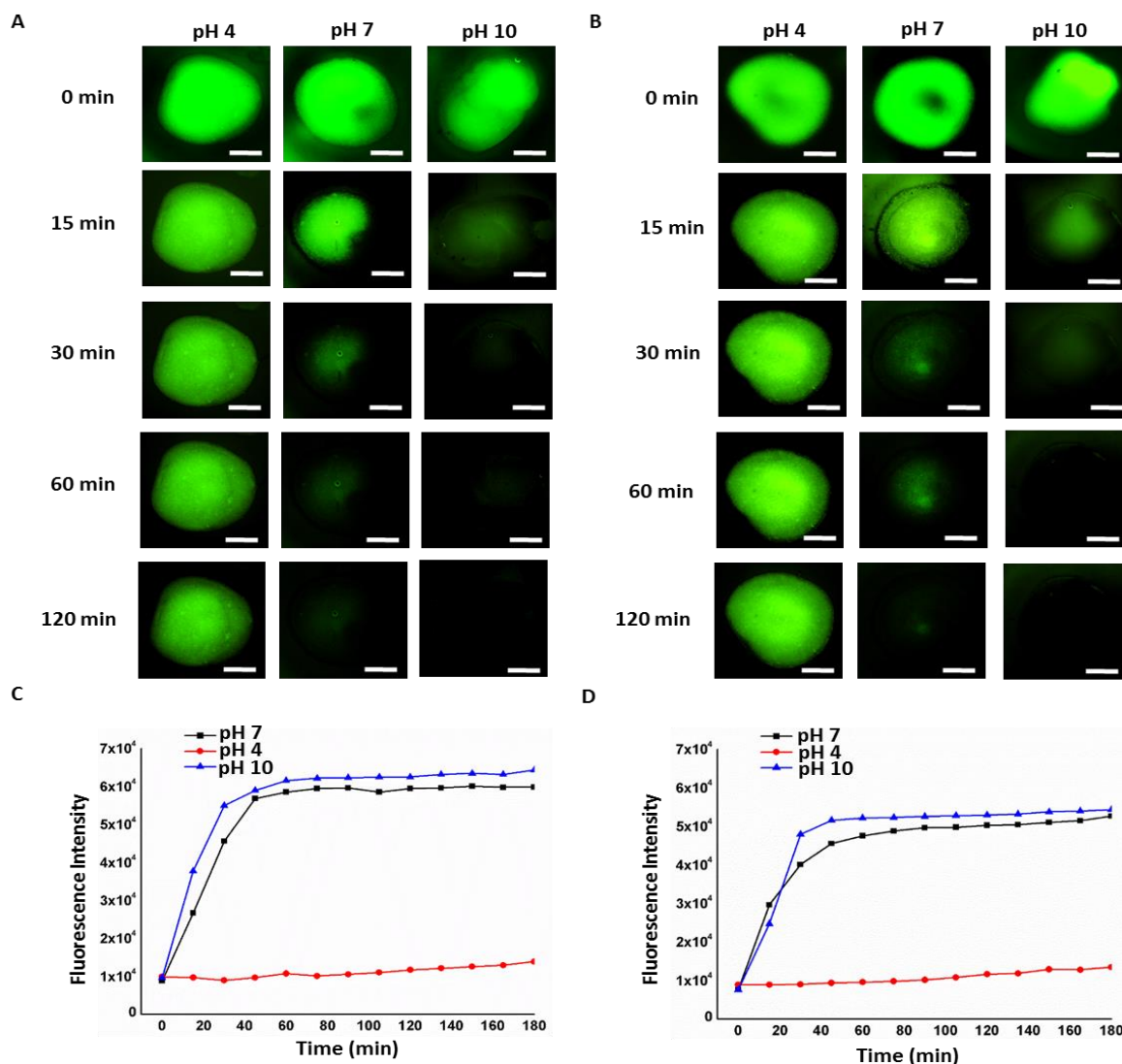
Figure 4. Cargo release from peptide-polymer membrane. (A) Fluorescent microscopic images of the membrane formed at 4$^\mathrm{o}$C after encapsulation of green Alexafluoro488 dye, when incubated at different pHs over time. Scale bar represents 500 μm, (B) Fluorescent microscopic image of the membrane formed at 30^{0}C after encapsulation of green Alexafluoro488 dye when incubated at different pHs over time. Scale bar represents 500 μm. Alexafluoro488 dye release kinetics over 3 h when immersed in buffers with different pHs (C) Membrane formed at 4^{0}C, (D) Membrane formed at 30^{0}C.

315   cytocompatibility of the membranes further by quantifying the percentage of live cells on the

316   membranes 3 days after seeding. An MTT assay of the cells seeded on the surface of the

317   membranes prepared both above and below T_t found to be greater than 90% cell viability

318   (Figure 3I). It should be noted that the adhesion and cytocompatibility of MC3T3-E1 cells on

319   membranes formed by ELP4 (an elastin-based protein without RGDS) and the peptide

320   FmocFFK, were very low, as observed from MTT analysis and fluorescence images (Figure

17

321 S16). These findings support the idea that cell adhesion and proliferation in the ELP5-

322 FmocFFK membranes is a result of the presence of RGDS sequence in ELP5.

323

ELP5-FmocFFK membranes can encapsulate and release dye in a pH-dependent fashion

325 Membranes formed at both 4 and 30 ^{0}C exhibited a decrease in storage modulus with increasing

326 pH. Lower value of storage modulus in alkaline pH compared to that of acidic pH suggested

327 that the interactions between the protein and the peptide molecules is weakened in alkaline

328 medium which results in overall lower mechanical rigidity. Herein we wanted to learn if this

329 pH dependent variation in mechanical rigidity of the membranes can be utilized towards

330 controlled release of bio-molecules. In order to study the controlled release properties,

331 Alexafluor 488 dye was encapsulated inside membranes and the rate of release at different pHs

332 was monitored over a period of 2 hours. No dye was released at pH 4 (acidic pH), but at neutral

333 pH 7, the dye was released from both the membranes within 1 hour (Figure 4A, B). When the

334 pH was raised further, the release was even faster and was essentially complete within 30 mins

335 (Figure 4C, D). Thus, there is a pH dependent dye release from both the membranes, prepared

336 above and below T_t, which can be explained by the pH dependent change in membrane

337 stability. However, the membranes remained intact after the complete release of the dye in

338 neutral and alkaline pH. These results demonstrate that the ELP5-FmocFFK membrane

339 systems could be suitable for encapsulation and pH dependent release of small bioactive

340 molecules.

341

342

343

18

CONCLUSION

We demonstrated the formation of stable ELP5-FmocFFK membranes prepared by

electrostatic interaction between an elastin-like protein and the short aromatic peptides. These

membranes are formed due to optimum hydrophilic and lipophilic balance in the short peptide

that can interact with both ordered and disordered forms of ELP. Similar to peptide amphiphile

-ELP system[17], the membrane are formed at temperatures above the conformational transition

temperature of the protein. Surprisingly only in the ELP5-FmocFFK system stable membrane

were form also below the conformational transition temperature. The membranes were found

to be robust and stable over a wide range of parameters, including time, temperature, pH, and

ultrasound energy. Microscopic analysis reveals minor differences in the composition of

membranes formed above or below the transition temperature. Furthermore, both types of

membranes support MC3T3-E1 preosteoblast cell adhesion, proliferation and display unique

pH dependent cargo release property which was not observed in previously reported

membranes. We can conclude that the short aromatic peptides overcome any conformational

restrictions of ELP and interacts with both ordered and disordered forms of the protein. The

novel robust macroscale hybrids produced offering new possibilities for controlling disorder

protein and improving future material design.

ASSOCIATED CONTENT

Supporting information contains all experimental details, Structure of the peptides, Peptide

concentration dependent membrane formation, Membrane picked up by twizers, Mass spectral

analysis, Stability of the peptide-polymer membranes with change in pH, Mechanical

properties of the membranes, Stability of the peptide-polymer membranes with change in

temperature, Stability of the peptide-polymer membranes under sonication, Media stability of

19

368 peptide-ELP4 membrane, Scanning electron microscopy image of cells on peptide-ELP4

369 membrane, In vitro biocompatibility on peptide-ELP4 membrane.

370

371

AUTHOR INFORMATIONS

373 **Corresponding Author:**

374 **Lihi-Adler-Abramovich -** Department of Oral Biology, The Goldschleger School of Dental
375 Medicine, Sackler Faculty of Medicine, Tel-Aviv University 69978, Israel.
376 The Centre for Nanoscience and Nanotechnology, Tel Aviv University, Tel Aviv, 6997801
377 Israel. orcid.org/0000-0003-3433-0625; Email: LihiA@tauex.tau.ac.il
378

379 **Authors:**

380 **Moumita Ghosh** - Department of Oral Biology, The Goldschleger School of Dental Medicine,
381 Sackler Faculty of Medicine, Tel-Aviv University 69978, Israel.
382 The Centre for Nanoscience and Nanotechnology, Tel Aviv University, Tel Aviv, 6997801
383 Israel.
384 Department of Chemistry, Techno India University, EM-4, EM Block, Sector V, Bidhannagar,
385 Kolkata, West Bengal 700091, India.
386 orcid.org/0000-0002-8049-7330
387

388 **Anna Majkowska** - School of Engineering & Materials Science, Queen Mary University of
389 London, London E1 4NS, U.K.
390 William Harvey Research Institute, Queen Mary University of London, London, EC1M 6BQ,
391 UK.
392

393 **Rajkumar Misra -** Department of Oral Biology, The Goldschleger School of Dental Medicine,
394 Sackler Faculty of Medicine, Tel-Aviv University 69978, Israel.
395 The Centre for Nanoscience and Nanotechnology, Tel Aviv University, Tel Aviv, 6997801
396 Israel.
397

398 **Santu Bera -** Department of Oral Biology, The Goldschleger School of Dental Medicine,
399 Sackler Faculty of Medicine, Tel-Aviv University 69978, Israel.
400 The Centre for Nanoscience and Nanotechnology, Tel Aviv University, Tel Aviv, 6997801
401 Israel.
402 orcid.org/0000-0002-4830-552X
403

404 **José Carlos Rodriguez-Cabello -** BIOFORGE Group, University of Valladolid, CIBER-
405 BBN, Valladolid 47011, Spain.

406

407 **Alvaro Mata -** School of Pharmacy, University of Nottingham, Nottingham NG7 2RD, UK.
408 Department of Chemical and Environmental Engineering, University of Nottingham,
409 Nottingham NG7 2RD, UK.
410 Biodiscovery Institute, University of Nottingham, Nottingham NG7 2RD, UK.

411

Acknowledgments

References:

427 (1) Simon, J. R.; Carroll, N. J.; Rubinstein, M.; Chilkoti, A.; López, G. P. Programming
428 molecular self-assembly of intrinsically disordered proteins containing sequences of low
429 complexity. *Nat. Chem.* **2017**, *9*, 509.

430 (2) Zhang, S. Fabrication of novel biomaterials through molecular self-assembly. *Nat.
431 Biotechnol*. **2003,** *21*, 1171.

432 (3) Siebler, C.; Erdmann, R. S.; Wennemers. H. Switchable proline derivatives: tuning the
433 conformational stability of the collagen triple helix by pH changes. *Angew. Chem. Int. Ed.*
434 **2014***, 53,* 10340 –10344.

435   (4) Zhang, S. Lipid-like self-assembling peptides. *Acc. Chem. Res. '***2012***, 45,* 2142–2150.

436   (5) Vepari, C.; Kaplan, D. L. Silk as a Biomaterial. *Prog Polym Sci*. **2007**, *32*, 991–1007.

437   (6) Li, Q.; Zhu, L.; Liu, R.; Huang, D.; Jin, X.; Che, N.; Li, Z.; Qu, X.; Kanga, H.; Huang, Y.
438   Biological stimuli responsive drug carriers based on keratin for triggerable drug delivery. *J.*
439   *Mater. Chem.* **2012**, *22*, 19964–19973.

440   (7) Scheuer, K.; Helbing, C.; Firkowska-Bodena, I.; Jandt, K. D. Self-assembled fibrinogen–
441   fibronectin hybrid protein nanofibers with medium-sensitive stability. *RSC Adv.* **2021***, 11,*
442   14113-14120.

443   (8) Dear, A. J.; Meisl, G.; Michaels, T. C. T.; Zimmermann, M. R.; Linse S.; Knowles, T. P.
444   J. The catalytic nature of protein aggregation. *J. Chem. Phys.* **2020**, *152*, 045101**.**

445   (9) Mendoza-Espinosa, P.; Garcı′a-Gonza′lez, V.; Moreno, A.; Castillo, R.; Mas-Oliva, J. *Mol*
446   *Cell Biochem* **2009,** *330*, 105–120.

447   (10) Ruff, K. M.; Roberts, S.; Chilkoti, A.; Pappu, R. V. Disorder-to-order conformational
448   transitions in protein structure and its relationship to disease. *J. Mol. Biol.* **2018**, *430*, 4619–
449   4635.

450   (11) Quiroz, F. G.; Li, N. K.; Roberts, S.; Weber, P.; Dzuricky, M.; Weitzhandler, I.; Yingling,
451   Y. G.; Chilkoti, A. Intrinsically disordered proteins access a range of hysteretic phase
452   separation behaviors. *Sci. Adv.* **2019**, *5*, eaax5177.

453   (12) Garaizar, A.; Sanchez-Burgos, I.; Collepardo-Guevara, R.; Espinosa, J. R. Expansion of
454   Intrinsically Disordered Proteins Increases the Range of Stability of Liquid-Liquid Phase
455   Separation. *Molecules* **2020,** *25*, 4705.

456   (13) Dignon, G. L.; Zheng, W.; Kim, Y. C.; Mittal, J. Temperature-Controlled Liquid-
457   Liquid Phase Separation of Disordered Proteins. *ACS Cent. Sci.* **2019**, *5*, 821−830.

458   (14) Martin, L.; Castro, E.; Ribeiro, A.; Alonso, M.; Rodriguez-Cabello, J. C. Temperature-
459   triggered self-assembly of elastin-like block co-recombinamers:the controlled formation of
460   micelles and vesicles in an aqueous médium. *Biomacromolecules* **2012**, *13*, 293–298.

461   (15) Rodriguez-Cabello, J. C.; Prieto, S.; Reguera, J.; Arias, F. J.; Ribeiro, A. Biofunctional
462   design of elastin-like polymers for advanced applications in nanobiotechnology. *J. Biomater.*
463   *Sci. Polym. Ed.* **2007**, *18*, 269–286.

464   (16) Almine, J. F.; Bax, D. V.; Mithieux, S. M.; Nivison-Smith, L.; Rnjak, J.; Waterhouse, A.;
465   Wise, S. G.; Weiss, A. S. Elastin-based materials. *Chem. Soc. Rev.* **2010**, *39*, 3371–3379.

466   (17) Inostroza-Brito, K. E.; Collin, E.; Siton-Mendelson, O.; Smith, K. H.; Monge-Marcet, A.;
467   Ferreira, D. S.; Rodríguez, R. P.; Alonso, M.; Rodríguez-Cabello, J. C.; Reis, F. Sagués, R. L.;
468   Botto, L.; Bitton, R.; Azevedo, H. S.; Mata, A. Co-assembly, spatiotemporal control and
469   morphogenesis of a hybrid protein-peptide system. *Nat. Chem.* **2015**, *7*, 897-904.

470   (18) Cheng, W.; Ding, Z.; Zheng, X.; Lu, Q.; Kong, X.; Zhou, X.; Lu, G.; Kaplan, D. L.
471   Injectable hydrogel systems with multiple biophysical and biochemical cues for bone
472   regeneration. *Biomater. Sci.*, **2020**, *8*, 2537–2548.

(19) Helbing, C.; Jandt, K. D. *Artificial Protein and Peptide Nanofibers, Woodhead Publishing,* 10.1016/B978-0-08-102850-6.00004-8.

(20) Reches, M.; Gazit, E. Casting metal nanowires within discrete self-assembled peptide nanotubes. *Science* **2003,** *300*, 625–627.

(21) Rufo, C. M. et al. Short peptides self-assemble to produce catalytic amyloids. *Nat. Chem.* **2014,** *6,* 303–309.

(22) Kim, S.; Kim, J. H.; Lee, J. S.; Park, C. B. Beta-Sheet-Forming, Self-Assembled Peptide Nanomaterials towards Optical, Energy, and Healthcare Applications. *Small* **2015***, 11,* 3623–3640.

(23) Tao, K.; Makam, P.; Aizen, R.; Gazit, E. Self-assembling peptide semiconductors. *Science* **2017,** *358*, eaam9756.

(24) Dasgupta, A.; Mondal, J.; Das, D. Peptide hydrogels. *RSC Adv.* **2013**, *3*, 9117-9149.

(25) Frederix, P. W. J. M.; Scott, G. G.; Abul-Haija, Y. M.; Kalafatovic, D.; Pappas, N. Javid, C. G.; Hunt, N. T.; Ulijn, R. V.; Tuttle, T. Exploring the sequence space for (tri-)peptide self-assembly to design and discover new hydrogels. *Nat. Chem.* **2015**, *7*, 30-37.

(26) Bera, S.; Mondal, S.; Xue, B.; Shimon, L. J. W.; Cao, Y.; Gazit, E. Rigid helical-like assemblies from a self-aggregating tripeptide. *Nat. Mater.* **2019**, *18*, 503-509.

(27) Okesola, B. O.; Mata, A. Multicomponent self-assembly as a tool to harness new properties from peptides and proteins in material design. *Chem. Soc. Rev.* **2018**, *47*, 3721-3736.

(28) Okesola, B. O.; Wu, Y.; Derkus, B.; Gani, S.; Wu, D.; Knani, D.; Smith, D. K.; Adams, D. J.; Mata, A. Supramolecular self-assembly to control structural and biological properties of multicomponent hydrogels. *Chem. Mater.* **2019**, *31*, 7883−7897.

(29) Makam, P.; Gazit, E. Minimalistic peptide supramolecular co-assembly: expanding the conformational space for nanotechnology. *Chem. Soc. Rev.* **2018**, *47*, 3406-3420.

(30) Okesola, B. O.; Lau, H. K.; Derkus, B., Boccorh, D. K.; Wu, Y.; Wark, A. W.; Kiick, K. L.; Mata, A. Covalent co-assembly between resilin-like polypeptide and peptide amphiphile into hydrogels with controlled nanostructure and improved mechanical properties. *Biomater. Sci.*, **2020**, *8*, 846–857.

(31) Halperin-Sternfeld, M.; Ghosh, M.; Sevostianov, R.; Grigoriants, I.; Adler-Abramovich, L. Molecular co-assembly as a strategy for synergistic improvement of the mechanical properties of hydrogels. *ChemComm.* **2017**, *53*, 9586-9589.

(32) Ghosh, M.; Bera, S.; Schiffmann, S.; Shimon, L. J. W.; Adler-Abramovich, L. Collagen-Inspired Helical Peptide Coassembly Forms a Rigid Hydrogel with Twisted Polyproline II Architecture. *ACS Nano,* **2020***, 14,* 9990–10000.

(33) Ghosh, M.; Halperin-Sternfeld, M.; Grigoriants, I.; Lee, J.; Nam, K. T.; Adler-Abramovich, L. Arginine-Presenting Peptide Hydrogels Decorated with Hydroxyapatite as Biomimetic Scaffolds for Bone Regeneration. *Biomacromolecules* **2017**, *18*, 3541-3550.

23

(34) Adler-Abramovich, L., Marco, P.; Arnon, Z. A.; Creasey, R. C. G.; Michaels, T. C. T.; Levin, A.; Scurr, D. J.; Roberts, C. J.; Knowles, T. P. J.; Tendler, S. J. B.; Gazit, E. Controlling the Physical Dimensions of Peptide Nanotubes by Supramolecular Polymer Coassembly. *ACS Nano* **2016**, *10*, 7436-7442.

(35) Wu, Y.; Okesola, B. O.; Xu, J.; Korotkin, I.; Berardo, A.; Corridori, I.; Brocchetti, F. L. P.; Kanczler, J.; Feng, J.; Li, W.; Shi, Y.; Farafonov, V.; Wang, Y.; Thompson, R. F.; Titirici, M. M.; Nerukh, D.; Karabasov, S.; Oreffo, R. O. C.; Carlos Rodriguez-Cabello, J.; Vozzi, G.; Azevedo, H. S.; Pugno, N. M.; Wang, W.; Mata, A. Disordered protein-graphene oxide co-assembly and supramolecular biofabrication of functional fluidic devices. *Nat. Commun* **2020**, *11*, 1182.

(36) Ustun Yaylaci, S.; Sardan Ekiz, M.; Arslan, E.; Can, N.; Kilic, E.; Ozkan, H.; Orujalipoor, I.; Ide, S.; Tekinay, A. B.; Guler, M. O. Supramolecular GAG-like Self-Assembled Glycopeptide Nanofibers Induce Chondrogenesis and Cartilage Regeneration. *Biomacromolecules*, **2016**, *17*, 679–689.

(37) Diaferia, C.; Morelli, G.; Accardo, A. Fmoc-diphenylalanine as a suitable building block for the preparation of hybrid materials and their potential applications. *J. Mater. Chem. B* **2019**, *7*, 5142-5155.

(38) Chen, L.; Revel, S.; Morris K.; Adams, D. J. Energy transfer in self-assembled dipeptide hydrogels. *Chem. Commun.*, **2010**, *46*, 4267.

(39) Wang, M.; Lv, Y.; Liu, X.; Qi, W.; Su, R.; He, Z. Enhancing the Activity of Peptide-Based Artificial Hydrolase with Catalytic Ser/His/Asp Triad and Molecular Imprinting. *ACS Appl. Mater. Interfaces*, **2016**, *8*, 14133–14141.

(40) Hudalla, G. A.; Sun, T.; Gasiorowski, J. Z.; Han, H.; Tian, Y. F.; Chong A. S.; Collier, J. H. Gradated assembly of multiple proteins into supramolecular nanomaterials. *Nat. Mater.*, **2014**, *13*, 829–836.

(41) Derkus, B.; Okesol, B. O.; Barrett, D. W.; D'Este, M.; Chowdhury, T. T.; Eglin, D.; Mata, A. Multicomponent hydrogels for the formation of vascularized bone-like constructs in vitro. *Acta Biomaterialia*, **2020**, *109*, 82–94.

(42) Hedegaard, C. L.; Redondo-Gómez, C.; Tan, B. Y.; Ng, K. W.; Loessner, D.; Mata, A. Peptide-protein coassembling matrices as a biomimetic 3D model of ovarian cáncer. *Sci. Adv.* **2020**, *6*, eabb3298.

(43) Capito, R. M.; Azevedo, H. S.; Velichko, Y. S.; Mata, A.; Stupp, S. I. Self-assembly of large and small molecules into hierarchically ordered sacs and membranes. *Science,* **2008**, *319*, 1812–1816.

(44) Chowa, L. W.; Bitton, R.; Webber, M. J.; Carvajal, D.; Shull, K. R.; Sharma, A. K.; Stupp, S. I. A bioactive self-assembled membrane to promote angiogenesis. *Biomaterials*, **2011**, *32*, 1574-1582.

(45) Behanna, H. A.; M. Donners, J. J. J.; Gordon, A. C.; Stupp, S. I. Coassembly of amphiphiles with opposite peptide polarities into nanofibers. *J. Am. Chem. Soc.* **2005**, *127*, 1193–1200.

552 (46) Inostroza-Brito, K. E.; Collin, E. C.; Majkowska, A.; Elsharkawy, S.; Rice, A.; del Río
553 Hernández, A. E.; Xiao, X.; Rodríguez-Cabello, J.; Mata, A. Cross-linking of a biopolymer-
554 peptide co-assembling system. *Acta Biomater.* **2017**, *58*, 80–89.

555 (47) Tejeda-Montes, E.; Smith, K. H.; Poch, M.; López-Bosque, M. J.; Martín, L.; Alonso, M.;
556 Engel, E.; Mata, A. Engineering membrane scaffolds with both physical and biomolecular
557 signalling. *Acta Biomater.* **2012**, *8*, 998–1009.

558 (48) González-Obeso, C.; González-Pérez, M.; Mano, J. F.; Alonso, M.; Rodríguez-Cabello, J.
559 C. *Complex* Morphogenesis by a Model Intrinsically Disordered Protein. *Small* **2020**, *16*,
560 2005191.

561